URL

Supporting Information for "Laboratory measurement of large-amplitude whistler pulses generated by fast magnetic reconnection"

Magnus A. Haw,[1] Byonghoon Seo,[1] Paul M. Bellan,[1]

Contents of this file

1. Text S1

2. Figures S1 to S6

Introduction The following describes the calculation of B & J from the quadprobe data and provides five additional figures. The first two figures plot typical images and wave measurements from a shot with magnetic reconnection and from a shot with no significant instabilities (e.g. straight jet case). The third figure plots a histogram of the maximum $\dot{B}$ (T/s) for the 23 measured wave pulses. The fourth figure provides an overview of the Langmuir probe measurement. The final figure is a plot of the wave pulse parameter space on the CMA diagram.

---

[1]Department of Applied Physics and
Materials Science, California Institute of
Technology, CA 91125

Text S1.

Calculation of B & J The tetrahedral arrangement allows a first order interpolation of the current density at the center of the tetrahedron. The current density is calculated by writing the $\mathbf{B}_i$ at each cluster as a Taylor expansion of $\mathbf{B_c}$ at the tetrahedron center,

$$\mathbf{B}_i = \mathbf{B}_c + (\vec{\nabla}\mathbf{B_c}) \cdot \mathbf{R}_i, \tag{1}$$

where the i subscript denotes a cluster index and $\mathbf{R}_i$ is the cluster location relative to the center of the tetrahedron. The following shows this equation written out for the B_x-component where $a = 2.2$ cm is the tetrahedron side length,

$$\overbrace{\begin{pmatrix} B_{0x} \\ B_{1x} \\ B_{2x} \\ B_{3x} \end{pmatrix}}^{\mathbf{A}} = \underbrace{\begin{pmatrix} 1 & 0 & 0 & \frac{-3a}{\sqrt{24}} \\ 1 & \frac{a}{\sqrt{3}} & 0 & \frac{a}{\sqrt{24}} \\ 1 & \frac{-a}{2\sqrt{3}} & \frac{a}{2} & \frac{a}{\sqrt{24}} \\ 1 & \frac{-a}{2\sqrt{3}} & \frac{-a}{2} & \frac{a}{\sqrt{24}} \end{pmatrix}}_{\mathbf{M}} \overbrace{\begin{pmatrix} B_{cx} \\ \frac{\partial B_{cx}}{\partial x} \\ \frac{\partial B_{cx}}{\partial y} \\ \frac{\partial B_{cx}}{\partial z} \end{pmatrix}}^{\mathbf{D}} \tag{2}$$

This equation can be inverted to recover the center value and center derivatives, $\mathbf{D} = \mathbf{M}^{-1} \cdot \mathbf{A}$. Repeating this calculation for the B_y and B_z components gives all the derivatives necessary to calculate the current density $\mathbf{J}$.

This first order approximation of $\mathbf{J}$ works best for wavelengths much larger than the 2.2 cm probe spacing. This limits accurate measurements of current density to wavelengths larger than $\sim$10 cm.

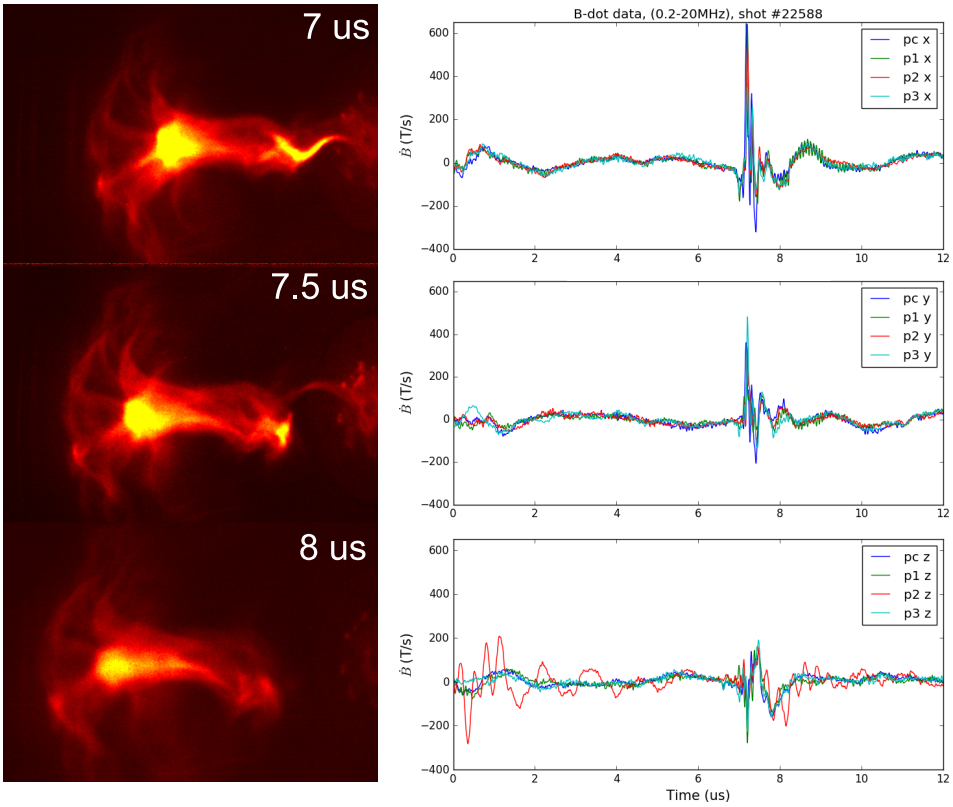

Figure S1. (Left) Image sequence for shot #22588 with fast reconnection induced by kink and Rayleigh-Taylor instabilities. Characteristic features are a helical perturbation and thinning of the jet axis before detachment (Right) Wave pulse measurements for the B_x, B_y, B_z components of each of the four clusters in the quadprobe.

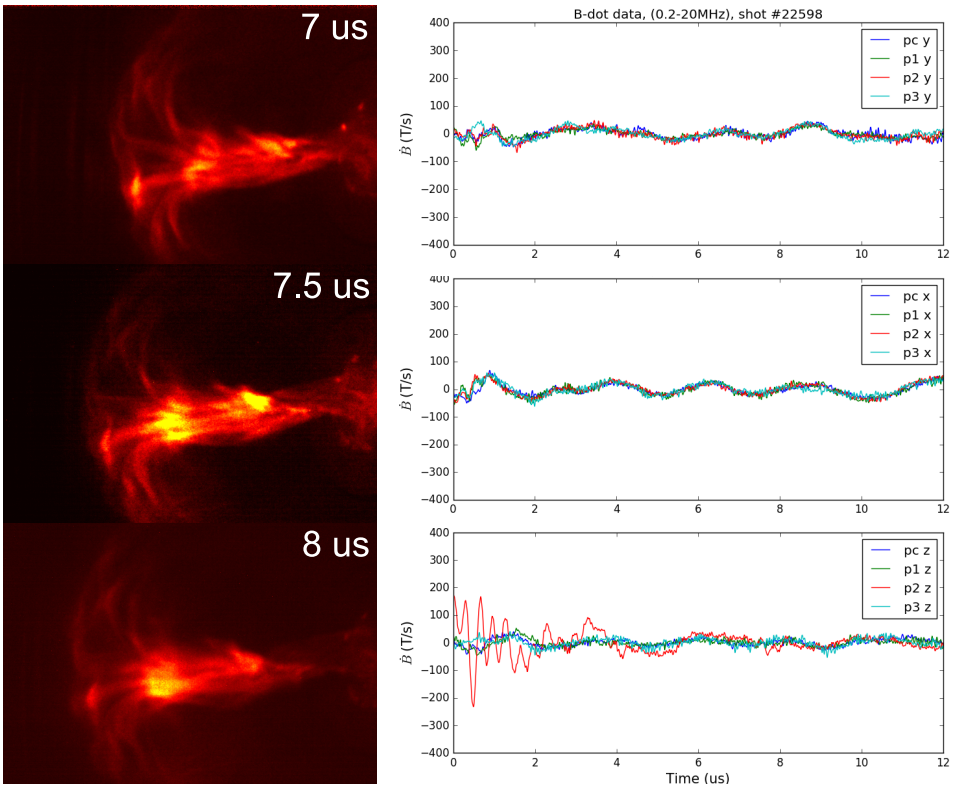

Figure S2. (Left) Image sequence for shot #22598, a straight jet case (i.e without significant kink or Rayleigh-Taylor instabilities). (Right) Typical quadprobe measurements for the B_x, B_y, B_z components of each of the four clusters in the quadprobe. There are no high frequency pulses observed for straight jet cases.

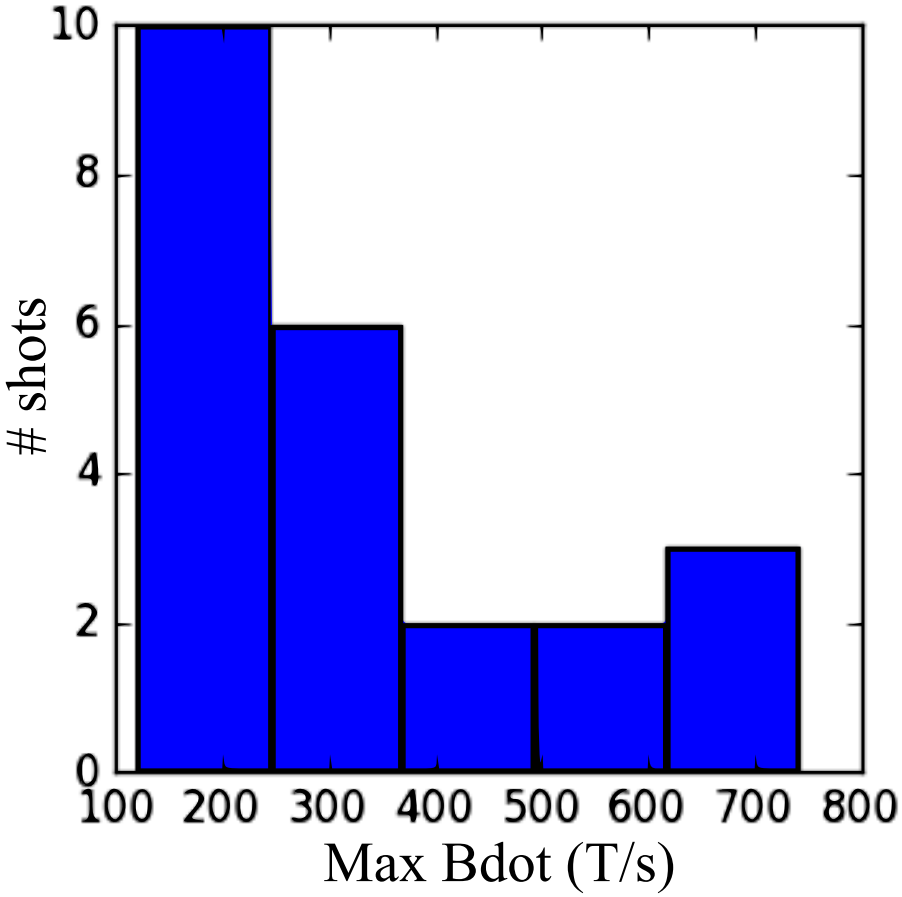

Figure S3. Histogram of maximum $\dot{B}$ (T/s) for the 23 observed wave pulses.

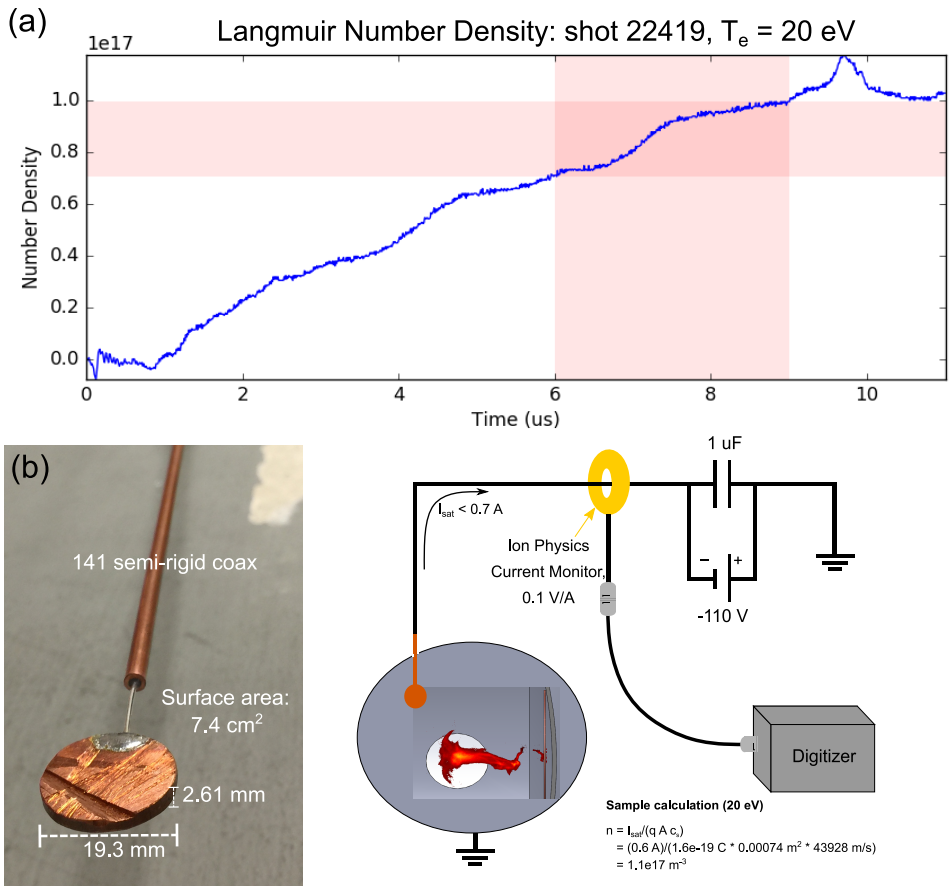

Figure S4. (a) Langmuir probe measurement of density as a function of time after plasma breakdown: $n = I/(c_s A q)$ where I is current, $c_s = \sqrt{\kappa_B T_e/m_i}$, A is area, and q is the elemental charge. (b) Image of Langmuir probe constructed from coin-like copper disk and 141 semi-rigid coax. (c) Circuit diagram for Langmuir probe. Probe is biased at -110 V by battery in parallel with a 1 μF capacitor. Ion physics current monitor gives an isolated current measurement and prevents ground loop noise. The probe draws less than 0.7 amps of current during the experiments.

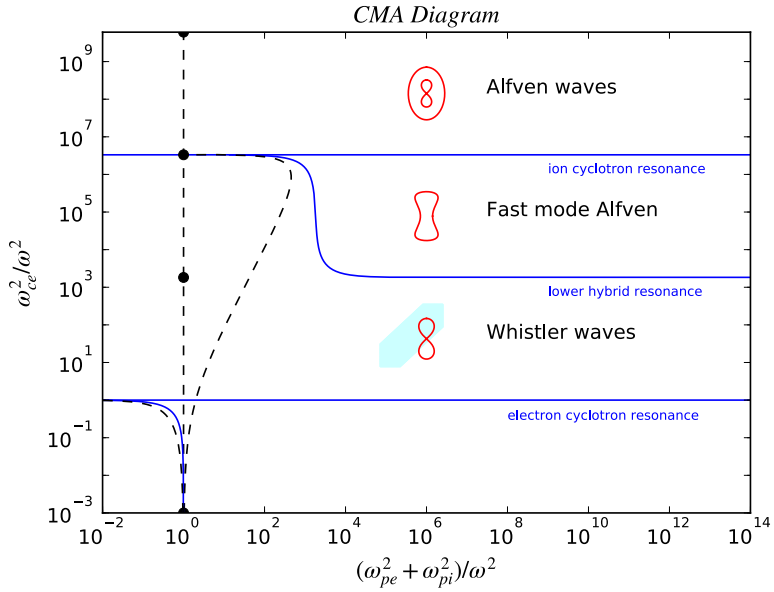

Figure S5. Plot of experimental parameter space on a Clemmow-Mullaly-Allis (CMA) diagram. The light blue region covers the range of wave pulse parameters: B = 0.001-0.002 T, n =0.9-2.8×10^{17} m^{-3}, and f = 3-10 MHz. Consequently, the observed wave pulses should be whistler modes since the parameters are well separated from both the lower hybrid and electron cyclotron resonances.

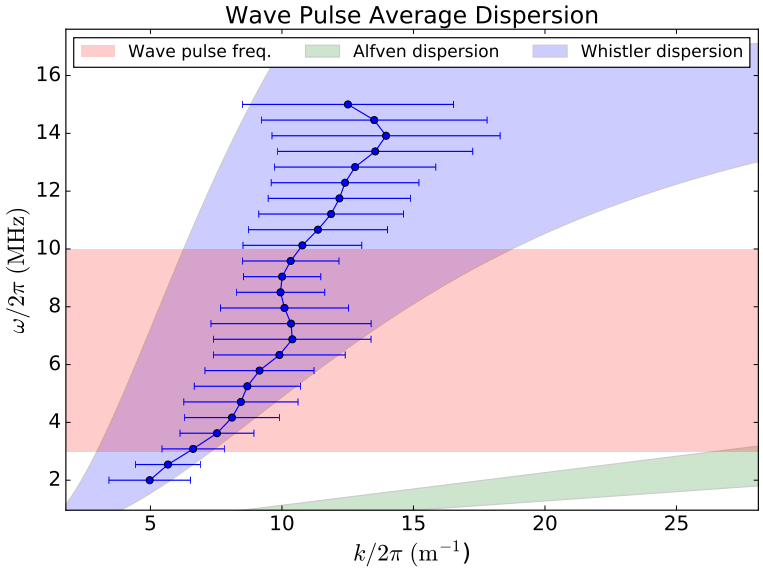

Figure S6. Plot of average $|k|$ from sample of 11 pulses with $\delta B/B > 0.01$. Error bars represent the standard deviation of the sample value at a given frequency. Whistler (blue) and Alfvén (green) dispersions are plotted for densities (0.9-2.8$\times 10^{17}$), oblique propagation (30-70°). The pink region covers the principal frequencies of the wave pulses.